Cluster Dynamical Mean Field Analysis of the Mott Transition

O. Parcollet and G. Biroli
Service de Physique Théorique, CEA Saclay, 91191 Gif-Sur-Yvette, France

G. Kotliar
Center for Materials Theory, Department of Physics and Astronomy, Rutgers University, Piscataway, New Jersey 08854, USA
(Received 1 September 2003; published 3 June 2004)

We investigate the Mott transition using a cluster extension of dynamical mean field theory (DMFT). In the absence of frustration we find no evidence for a finite temperature Mott transition. Instead, in a frustrated model, we observe signatures of a finite temperature Mott critical point in agreement with experimental studies of κ organics and with single-site DMFT. As the Mott transition is approached, a clear momentum dependence of the electron lifetime develops on the Fermi surface with the formation of cold regions along the diagonal direction of the Brillouin zone. Furthermore, the variation of the effective mass is no longer equal to the inverse of the quasiparticle residue, as in DMFT, and is reduced approaching the Mott transition.

DOI: 10.1103/PhysRevLett.92.226402 PACS numbers: 71.10.–w, 71.30.+h

The Mott transition is one of the central issues in the physics of strongly correlated electron systems. Great theoretical progress in this area has been achieved using dynamical mean field theory (DMFT) [1]. In spite of these successes, the single-site DMFT approach has several limitations due to the k independence of the self-energy: variations of the quasiparticle residue, the quasiparticle lifetime, and the effective mass along the Fermi surface are absent. Moreover, some orders involving several sites like d-wave superconductivity cannot be described. Furthermore, single-site DMFT does not capture the effects of the magnetic exchange interaction on the single particle properties in the paramagnetic phase. This is potentially a singular perturbation, which can bring substantially new effects. Hence the question of whether the Mott transition survives beyond the single-site mean field approximation and how it is modified by short-range magnetic correlations is among the most pressing questions in the field.

These questions can now be addressed using cluster extensions of DMFT [2,3]. In this Letter we report a study of the cellular DMFT (CDMFT) approximation [3] on a 2×2 square cluster of the one-band Hubbard model on a square lattice with and without frustration, solving the CDMFT equations with the quantum Monte Carlo (QMC) method. In the unfrustrated model, the finite temperature Mott transition is precluded by antiferromagnetic (AFM) order. However, if the frustration is big enough to destroy this order, we show the existence of a Mott transition which is in agreement with the DMFT scenario and displays, at the same time, new physical effects due to the k dependence of the self-energy in the cluster method. In particular, we observe the appearance of different behavior of the one electron spectral function in different regions of the Fermi surface. This behavior, out of reach of single-site DMFT, is very important since observed in the photoemission experiments [4,5] of cuprate superconductors.

The one-band Hubbard model on a two-dimensional square lattice with hopping $t_{i,j}$ and Hubbard repulsion U reads:

$$H = -\sum_{i,j,\sigma} t_{i,j} c^\dagger_{i,\sigma} c_{j,\sigma} + \sum_i U\left(n_{i\uparrow} - \frac{1}{2}\right)\left(n_{i\downarrow} - \frac{1}{2}\right), \quad (1)$$

where $\sigma = \uparrow, \downarrow$ is the spin index and $c^\dagger_{i,\sigma}$ and $c_{j,\sigma}$ denote the electron operators. The bare one electron dispersion is given by $E_k = -2t[\cos(k_x) + \cos(k_y)] - 2t' \cos(k_x + k_y)$. We analyze both the unfrustrated model $t' = 0$ and the strongly frustrated one $t' \approx t$, where the antiferromagnetic order is expected to be destroyed by frustration [6]. We take $D \equiv 4t = 1$. This type of anisotropic band structure is particularly relevant for the study of organic materials such as κ-(BEDT-TTF)$_2X$ (see, e.g., [7]).

Within CDMFT we divide the lattice in a superlattice of 2×2 squares and we basically solve the DMFT equations applied to the superlattice [3](see Fig. 1). Starting from an effective action containing a Weiss dynamical field G_0 one computes by QMC (Hirsch-Fye algorithm) a local cluster propagator and a cluster self-energy (which are 4×4 matrices). The Weiss field is then recomputed using the Dyson equation

$$G_0^{-1}(i\omega_n) = \left(\sum_K \frac{1}{i\omega_n + \mu - \hat{t}(K) - \Sigma(i\omega_n)}\right)^{-1} + \Sigma(i\omega_n),$$

where K is in the reduced Brillouin zone of the superlattice, $\hat{t}$ is the hopping matrix for the superlattice, and μ is the chemical potential. This procedure is iterated until convergence is reached. In our QMC runs we use 30 000–300 000 QMC sweeps and a number of time slices $L \approx \beta U$. Finally, let us recall that in CDMFT, the lattice self-energy is different from the cluster self-energy Σ and reads [3] here (k is in the Brillouin zone):

 © 2004 The American Physical Society

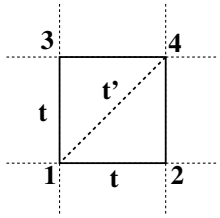

FIG. 1. The real space cluster and labeling conventions.

$$\Sigma^{\mathrm{latt}}(k) = \frac{1}{4}\sum_{i=1}^{4}\Sigma_{ii} + \frac{1}{2}[(\Sigma_{12}+\Sigma_{34})\cos(k_x) + (\Sigma_{24}+\Sigma_{13})\cos(k_y) + \Sigma_{14}\cos(k_x+k_y) + \Sigma_{23}\cos(k_x-k_y)].$$

Let us first focus on the unfrustrated case ($t' = 0$) at half-filling (see also [8–11]). We computed the Néel temperature, corresponding to the continuous onset of an antiferromagnetic solution, as a function of U. Our result is similar, even quantitatively, to the one obtained in a DMFT study of the bipartite half-filled Bethe lattice [1]. In particular the AFM transition takes place at a quite high temperature, precluding a finite temperature DMFT-like Mott transition (i.e., a first order transition ending at a finite temperature critical point).

Let us emphasize a major difference between single-site and cluster methods. In DMFT, the paramagnetic equations (i.e., the equations with enforced spin symmetry) are the same for the bipartite half-filled Bethe lattice and for a fully frustrated infinite dimensional model [1]. Therefore the study of the Mott transition can be performed analyzing the paramagnetic solution in the AFM part of the phase diagram. On the contrary, in cluster methods, the paramagnetic equations are not the equations of such a simple fully frustrated model. Because of the quantum short-range fluctuations existing inside the cluster, studying the paramagnetic solution for parameters where an ordered solution exists is unphysical. Indeed, if one forces the symmetry and follows the paramagnetic CDMFT solution inside the AFM region, a pseudogap opens because of the Slater mechanism. Some previous works have focused on increasing the cluster size [8,9]. The Néel temperature then decreases to 0, but the $T = 0$ AFM order can still induce long-range fluctuations at finite temperature and open a pseudogap.

On the contrary, in this Letter we analyze a *strongly frustrated* Hubbard model with a 2×2 cluster. In the following, we will take $t'/t = 1$. This frustration is big enough to destroy the AFM order, at least for intermediate temperatures $T/D > 0.02$ where we have performed QMC computations. In fact, we observe unambiguous signatures of a finite temperature Mott transition similar to the single-site DMFT case. In Fig. 2 we present the imaginary parts of the on-site cluster self-energy and propagator Σ''_{11} and G''_{11}, for different values of U and

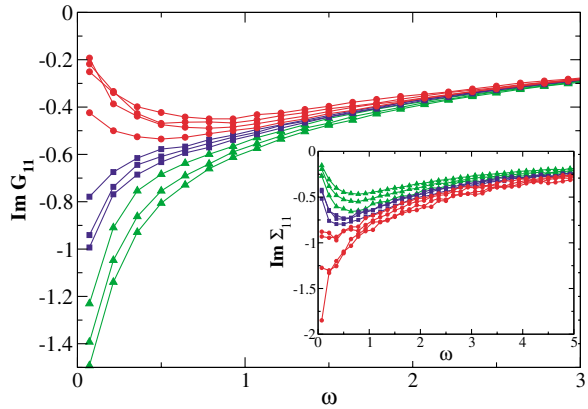

FIG. 2 (color online). Imaginary part of the on-site propagator and of the on-site self-energy (inset) in Matsubara frequencies for $U/D = 2, 2.1, 2.2$ [(green) curves with triangles], $U/D = 2.25, 2.29, 2.31$ [(blue) curves with squares], $U/D = 2.34, 2.43, 2.5$ [(red) curves with circles], and $T/D = 1/44$.

as a function of the Matsubara frequencies. For $U/D < 2.2$ and small ω_n, we observe a metallic behavior: $\Sigma''_{11}(i\omega_n) \sim (1 - \frac{1}{Z})\omega_n$. When $\omega_n \to 0$, the imaginary part of the on-site self-energy increases linearly, while G''_{11} decreases to a constant. This is the behavior characteristic of a Fermi liquid with a decreasing quasiparticle residue Z and a finite density of states at zero frequency. For $U/D > 2.34$ the behavior is clearly different: when ω_n decreases to 0, Σ''_{11} decreases while G''_{11} increases. This is characteristic of an insulating phase with a (pseudo)gap in the density of states. These results show clearly the crossover from a metallic to an insulating regime, similar to DMFT [1]. Furthermore, we have found indications of the existence of a finite temperature Mott critical point, located around $U_c/D \simeq 2.3$–2.4 and $T_c/D \simeq 1/44$. In Fig. 3, we present the double occupation $d_{\mathrm{occ}} \equiv \frac{1}{4}\sum_{i=0}^{4}\langle n_{i\uparrow}n_{i\downarrow}\rangle$ as a function of U for various temperatures. It presents a singular behavior similar to the one found in [12] for DMFT. Furthermore, the solution of the CDMFT equations displays a numerical "critical slowing down" around U_c, T_c. This is natural around a second order transition where new solutions appear continuously.

Let us now turn to the new aspects of the Mott transition that one can get with cluster methods and that are excluded from the beginning within a DMFT analysis. As discussed previously, they are encoded into the k dependence of the lattice self-energy. First, let us focus on the Fermi surface that can be located analyzing the maxima, as a function of k, of the spectral weight at zero frequency $A(k, \omega = 0) \approx \frac{1}{\pi}\lim_{\omega_n \to 0}\mathrm{Im}G(k, i\omega_n)$. Since the QMC method produces *finite temperature* data in imaginary time, the self-energy at zero frequency is estimated by a linear extrapolation toward zero from the first two Matsubara frequencies. In Fig. 4 we present $A(k, \omega = 0)$ for two metallic cases $U = 2.0, 2.25$. The Fermi surface is only weakly renormalized compared to the $U = 0$ value.

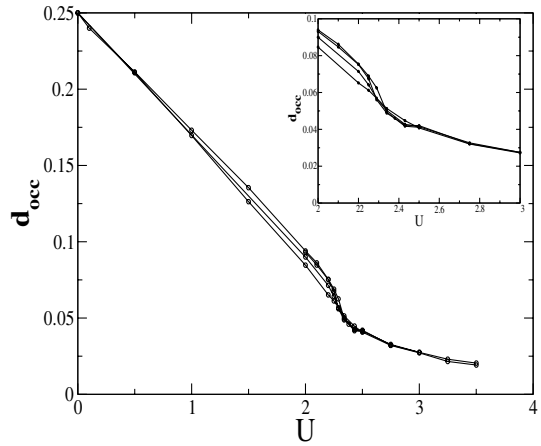

FIG. 3. Double occupancy as a function of U/D. The curves correspond (from bottom to top) to $T/D = 1/20, 1/30, 1/40, 1/44$.

Furthermore, the right-hand part of Fig. 4 shows that as the Mott transition is approached the regions along the diagonal are characterized by a larger spectral intensity, thus a bigger electronic lifetime, than along the $(0, \pi)$ directions. Note that the existence of hot and cold spots along the Fermi surface have been the subject of intensive discussions in the cuprate literature [13].

The mechanism for the momentum differentiation in our CDMFT study is as follows. When U increases, three sets of curves can be distinguished: for $U = 2, 2.1, 2.2$ (green) curves with triangles in Figs. 2 and 5, the on-site lattice self-energy exhibits metallic behavior, while the off-diagonal elements are very weak, leading to a DMFT-like result and to the $A(k, \omega = 0)$ plotted on the left-hand side in Fig. 4. For $U/D = 2.25, 2.29, 2.31$ [(blue) curves with squares], Σ_{11} is still metalliclike but the Σ''_{14}, Σ''_{23} are not negligible (see Fig. 5). We will refer to these points as the "intermediate region." For the largest U/D [2.34, 2.43, 2.5, (red) curves with circles], the system is a finite temperature Mott insulator. In this regime the real part of Σ_{14} and Σ_{23}, which can be thought of as a renormalization of the hopping matrix elements allowing the propagation of a hole without disturbing the antiferromagnetic background, become large and have a sign such that it tends to restore the square symmetry of the lattice. In the intermediate region, Σ''_{14} and Σ''_{23} become large and of comparable magnitude. This is a remarkable and unexpected effect, since the bare hopping amplitude between the 1, 4 and the 2, 3 sites are very different (0 and 0.25) in our model. Hence, using the approximation $\Sigma''_{14} \approx \Sigma''_{23}$, the anisotropy of the electron lifetime stems from $\Sigma''_{14} \cos(k_x) \cos(k_y)$. This quantity is maximum and negative around $(0, \pi)$ and $(\pi, 0)$ (hot spots) and is a minimum, i.e., zero, at the diagonal $(\pi/2, \pi/2)$ (cold spots) and leads to the curves plotted on the right-hand side in Fig. 4. Note, however, that this is an intermediate temperature effect. Indeed, a scenario where, at zero temperature and $\omega \to 0$, $\Sigma''_{11} \to 0$ and $\Sigma''_{14} \sim$ const [this would lead to a non-Fermi-liquid behavior more pronounced around $(0, \pi)$ and $(\pi, 0)$] is forbidden by causality (and thus by CDMFT): Σ'' has to be negative as a matrix for all ω, but if $\Sigma''_{11}(\omega = 0) = 0$ and $\Sigma''_{14}(\omega = 0) < 0$, the submatrix Σ_{ij} with $i, j \in \{1, 4\}$ would not be negative.

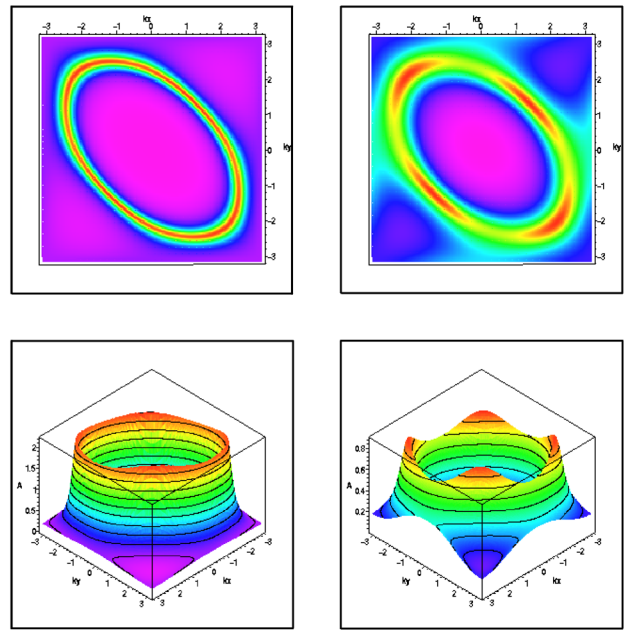

FIG. 4 (color online). Distribution of low energy spectral weight in k space $A(k, \omega = 0)$ for $T/D = 1/44$, $U/D = 2.0$ (left-hand panel) and $U/D = 2.25$ (right-hand panel). The top panels are color plots to see the Fermi surface and the bottom panels are 3D plots to see the variation of A. For intermediate U, cold and hot regions are visible around $(\frac{\pi}{2}, \frac{\pi}{2})$ and $(\pi, 0)$, respectively.

More refined quantities are the variation of the quasiparticle residue and the effective mass on the Fermi surface. We find that quasiparticle residue decreases with U, roughly linearly and becomes small near $U \approx U_c$, as in DMFT. However, since it involves the derivatives of the analytically continued self-energy, it cannot be evaluated within our QMC results with

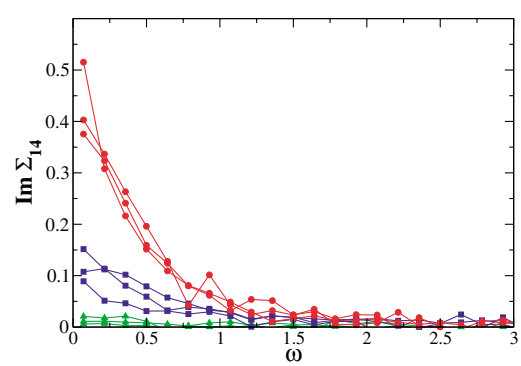

FIG. 5 (color online). Imaginary part of Σ_{14} for $T/D = 1/44$ and $U/D = 2, 2.1, 2.2$ [(green) curves with triangles], $U/D = 2.25, 2.29, 2.31$ [(blue) curves with squares], $U/D = 2.34, 2.43, 2.5$ [(red) curves with circles], and $T/D = 1/44$.

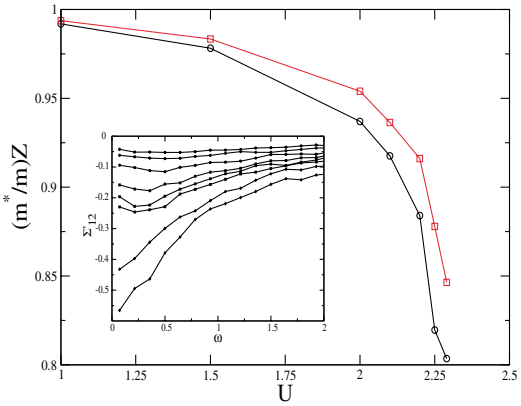

FIG. 6 (color online). $Z\frac{m^*}{m}$ as a function of U at $\beta D = 44$. Top (bottom) curve corresponds to the hot (cold) point. Inset: Σ'_{12} vs ω_n for $U/D = 2, 2.1, 2.2, 2.25, 2.29, 2.31$ (from top to bottom) and $T/D = 1/44$.

enough precision to differentiate the behavior of Z in the hot and cold region. On the other hand, an interesting physical quantity, which can be reliably extracted from the real part of the self-energy at zero frequency, is

$$Z\frac{m^*}{m} = \frac{1}{1 + \frac{d\Sigma'(k,0)}{dk_\perp} / \frac{dE_k}{dk_\perp}},$$

where m^* and m are, respectively, the renormalized and the bare effective mass, k is along the Fermi surface, and $\frac{d}{dk_\perp}$ means the derivative perpendicular to the Fermi surface. $\frac{m^*}{m}Z$ is plotted in Fig. 6 for $\beta D = 44$ as a function of U for the hot and cold points. Note that $\frac{m^*}{m}Z$ is always equal to 1 in single-site DMFT because of the k independence of the self-energy. Instead, within CDMFT we find that it decreases as we approach the Mott transition mainly because of the increase in modulus of the real part of Σ_{12} at zero frequency; see inset of Fig. 6. This leads to a contribution to the k-dependent renormalization of the effective mass which tends to counterbalance the increase of $1/Z$. Whether the effective mass at low temperatures remains finite as the Mott point is approached as in the large N studies of Ref. [14], or whether it diverges in an albeit weaker fashion than in DMFT, remains an open question which will require a lower temperature study.

Finally, analyzing the density of states using the maximum entropy [15] analytic continuation procedure, we have found that the quasiparticle peak found in DMFT in the metallic region is split near the Mott transition into two peaks, giving rise to a pseudogap.

To summarize, we found that the Mott transition, prevented by AFM order in the unfrustrated model, is present in the frustrated case. The single-site DMFT scenario characterized by a finite temperature Mott end point is compatible with our data. At low temperature a substantial k dependence of the self-energy shows up and regions with significant variation of the electron lifetime as a function of k appear. Raising the temperature, the k dependence of the self-energy gets weaker, and single-site DMFT becomes more accurate. Our analysis has been performed on a model relevant to the quasi-two-dimensional materials of the κ family [16,17]. Indeed, in Ref. [18] the Mott transition has been recently driven by pressure. It would be very interesting to carry out angle resolved photoemission experiments in these materials to verify our theoretical predictions, regarding the strong momentum dependence of the lifetimes. We conjecture that this differentiation in momentum space is more general than the model we studied, and is a direct consequence of the proximity to the Mott transition. Indeed it would be interesting to perform a similar study in a doped and isotropically frustrated Hubbard model relevant for high-T_c superconductors.

G. B. and O. P. are supported by an "ACI" grant of the French Minister of Research. The computations were carried out at the RUPC cluster at Rutgers.

[1] A. Georges, G. Kotliar, W. Krauth, and M. J. Rozenberg, Rev. Mod. Phys. **68**, 13 (1996).
[2] T. Maier, M. Jarrell, T. Pruschke, and J. Keller, Eur. Phys. J. B **13**, 613 (2000); M. H. Hettler, A. N. Tahvildar-Zadeh, M. Jarrell, T. Pruschke, and H. R. Krishnamurthy, Phys. Rev. B **58**, R7475 (1998).
[3] G. Kotliar, S. Y. Savrasov, G. Pálsson, and G. Biroli, Phys. Rev. Lett. **87**, 186401 (2001); G. Biroli, O. Parcollet, and G. Kotliar, cond-mat/0307587 [Phys. Rev. B (to be published)].
[4] H. Ding *et al.*, Nature (London) **382**, 51 (1996).
[5] A. G. Loeser *et al.*, Science **273**, 325 (1996).
[6] J. Merino, R. H. McKenzie, J. B. Marston, and C. H. Chung, J. Phys. Condens. Matter **11**, 2965 (1999).
[7] K. Kuroki and H. Aoki, Phys. Rev. B **60**, 3060 (1999).
[8] S. Moukouri and M. Jarrell, Phys. Rev. Lett. **87**, 167010 (2001); M. Jarrell, T. Maier, C. Huscroft, and S. Moukouri, Phys. Rev. B **64**, 195130 (2001).
[9] B. Kyung, J. S. Landry, D. Poulin, and A. S. Tremblay, Phys. Rev. Lett. **90**, 099702 (2003).
[10] K. Haujle *et al.*, Phys. Rev. Lett. **89**, 236402 (2002).
[11] T. Stanescu and P. Phillips, Phys. Rev. Lett. **91**, 017002 (2003).
[12] M. J. Rozenberg, R. Chitra, and G. Kotliar, Phys. Rev. Lett. **83**, 3498 (1999).
[13] R. Hlublina and T. M. Rice, Phys. Rev. B **51**, 9253 (1995); A. T. Zheleznyak *et al.*, Phys. Rev. B **57**, 3089 (1998); L. B. Ioffe and A. J. Millis, Phys. Rev. B **58**, 11 631 (1995); A. Perali, M. Sindel, and G. Kotliar, Eur. Phys. J. B **24**, 487 (2001).
[14] M. Grilli and G. Kotliar, Phys. Rev. Lett. **64**, 1170 (1990).
[15] M. Jarrell and J. E. Gubernatis, Phys. Rep. **269**, 133 (1996).
[16] Y. Shimizu *et al.*, Phys. Rev. Lett. **91**, 107001 (2003); H. Morita, S. Watanabe, and M. Imada, J. Phys. Soc. Jpn. **71** , 2109 (2002).
[17] P. Limelette *et al.*, Phys. Rev. Lett. **91**, 016401 (2003); R. H. McKenzie, Science **278**, 820 (1997); S. Lefebvre *et al.*, Phys. Rev. Lett. **85**, 5420 (2000).